Author/s:
Hejazi, MA;Tong, W;Stacey, A;Sun, SH;Yunzab, M;Almasi, A;Jung, YJ;Meffin, H;Fox, K;Edalati, K;Nadarajah, A;Prawer, S;Ibbotson, MR;Garrett, DJ

Title:
High Fidelity Bidirectional Neural Interfacing with Carbon Fiber Microelectrodes Coated with Boron-Doped Carbon Nanowalls: An Acute Study

Date:
2020-12-01

Citation:
Hejazi, M. A., Tong, W., Stacey, A., Sun, S. H., Yunzab, M., Almasi, A., Jung, Y. J., Meffin, H., Fox, K., Edalati, K., Nadarajah, A., Prawer, S., Ibbotson, M. R. & Garrett, D. J. (2020). High Fidelity Bidirectional Neural Interfacing with Carbon Fiber Microelectrodes Coated with Boron-Doped Carbon Nanowalls: An Acute Study. Advanced Functional Materials, 30 (52), https://doi.org/10.1002/adfm.202006101.

Persistent Link:
https://hdl.handle.net/11343/276334

High Fidelity, Bidirectional Neural Interfacing with Carbon Fiber Microelectrodes Coated with Boron-doped Carbon Nanowalls: an Acute Study

Maryam A. Hejazi, Wei Tong, Alastair Stacey, Shi H. Sun, Molis Yunzab, Ali Almasi, Young Jun Jung, Hamish Meffin, Kate Fox, Khatereh Edalati, Athavan Nadarajah, Steven Prawer, Michael R. Ibbotson, David. J Garrett*

M. A. Hejazi, Dr. W. Tong, Dr. A. Stacey, K. Edalati, Dr. A. Nadarajah, Prof. S. Prawer, Prof. D. J. Garrett

School of Physics, University of Melbourne, Parkville, Victoria, 3010, Australia

E-mail: wei.tong@unimelb.edu.au

Dr. W. Tong, S. H. Sun, Dr. M. Yunzab, Dr. A. Almasi, Y. J. Jung, Dr. H. Meffin, Prof. M. R. Ibbotson

National Vision Research Institute, Australian College of Optometry, Carlton, Victoria, 3053, Australia

Dr. W. Tong, Y. J. Jung, Dr. H. Meffin, Prof. M. R. Ibbotson

Department of Optometry and Vision Sciences, University of Melbourne, Parkville, Victoria, 3010, Australia

Dr. A. Stacey

School of Science, RMIT University, Melbourne, Victoria, 3000, Australia

Prof. K. Fox, Prof. D. J. Garrett

School of Engineering, RMIT University, Melbourne, Victoria, 3000, Australia

Prof. K. Fox

Center for Additive Manufacturing, RMIT University, Melbourne, Victoria, 3000, Australia

Keywords: carbon fiber, carbon nanowall, implantable, stimulation, recording.

Abstract

Implantable electrodes that can communicate with a small, selective group of neurons via both neural stimulation and recording are critical for the development of advanced neuroprosthetic devices. Microfiber electrodes with neuron-scale cross sections have the potential to improve the spatial resolution for both stimulation and recording, while minimizing the chronic inflammation response after implantation. In this work, we fabricated glass insulated microfiber electrodes by coating carbon fibers with boron-doped carbon nanowalls. The coating significantly improved the electrochemical properties of carbon fibers, leading to a charge injection capacity of 7.82 ± 0.35 mC cm^{-2}, whilst retaining good flexibility, stability and biocompatibility. When used for neural interfacing, the coated microelectrodes successfully elicited localized stimulation responses in explanted retina, and were also able to detect signals from single neurons, *in vivo* with a signal-to-noise ratio as high as 6.7 in an acute study. This is the first report of using carbon nanowall coated carbon fibers for neural interfacing.

1. Introduction

The trends in implantable neuroprosthetics are towards devices that are capable of stimulating and recording from individual or a small group of neurons[1]. These devices require electrodes to record neural signals with high fidelity, while still having the capacity to safely deliver sufficient electrical charge to elicit responses from a small volume of neural tissue. Today, most neuroprosthetic devices communicate with the nervous system in one-way, by either sending or reading out information. Novel microelectrode technologies that enable effective bidirectional communication will advance neuroscience research and many emerging therapies for neurological diseases.

A robust, high-fidelity neural interface can benefit significantly from the use of microfiber electrodes, which have cross-section diameters of about 10 μm, comparable to neuronal soma sizes[2]. Here, high-fidelity is defined as the ability to capture detailed, single unit spike activity with high spatial

resolution. Neuron-scale electrodes are expected to be able to evoke localized neural responses due to more confined electric fields. Also, the smaller recording sites improve the signal-to-noise ratio (SNR) of single-unit recordings, by better discriminating the signals of target neurons from the undesired background noise due to distant neuronal activity[3]. For chronic applications, a sustained reactive response to the insertion of the electrode is a major concern, which leads to the formation of glial scars around the implanted electrodes[1b]. Although the insertion injury cannot be avoided completely, the microfiber electrodes have been demonstrated to reduce glial scarring and neuronal loss[2b-d]. This scarring and neuronal loss is reduced by reducing the size of the insertion sites, and also by the inherent flexibility of microfiber electrodes, which leads to better mechanical compliance between electrodes and tissue[2b-d].

Electrode miniaturization, however, requires improvements in electrode materials due to decreased geometric surface area[4]. During neural stimulation, a limited amount of electric charge can be injected from the electrodes to the neural tissue before exceeding the water electrolysis potential range[4] and causing damage to neural tissue. For smaller electrodes, electrochemical capacitance decreases due to reduced surface area; therefore, the electrodes may not be able to inject sufficient charge to elicit neural responses[4]. Smaller electrodes also have larger electrochemical impedance[1b]. Increased impedance leads to higher noise during recording, making it difficult to detect the signals from the target neurons[1b, 5]. To overcome these difficulties, coating the fibers with materials that possess large effective surface areas can help[2c, 2e, 2f, 6]. However, this coating material must also be conductive, biocompatible, stable and, ideally, flexible. Most coating technologies have been designed to increase the effective surface area of electrodes on planar arrays. Finding a method to create a uniform coating on the fibers with neuron-scale dimension, which at the same time increases

the effective surface area, does not peel or crack upon bending and is electrochemically stable has been a materials-science challenge.

Carbon fibers (CF) are commonly used in the form of microfiber electrodes for neural interfacing[7]. These electrodes, with diameters of about 7 µm, display good flexibility and have been previously demonstrated to be effective electrodes for neural recording[7] and neurotransmitter sensing[8]. However, due to their small surface area, additional coatings are required for neural stimulation. Several coating materials have previously been used, including iridium oxide[6b], conductive polymers such as PEDOT:PSS[2e, 2f, 6a], and our recent report of nitrogen included ultrananocrystalline diamond (N-UNCD)[9]. All these coating materials improved the electrode charge injection capacity, however the stability of the coatings upon bending and under repetitive stimulation has rarely been demonstrated.

Here, we report a new coating material, boron-doped carbon nanowalls (B-CNW), for improving the performance of CF microelectrodes for neural interfacing. Carbon nanowalls (CNW) are two dimensional graphitic platelets, each composed of a few layers of graphene and typically oriented vertically on a substrate[10]. In the present work, we show that the B-CNW coating increases the effective surface area of the electrodes, and therefore their electrochemical properties including charge injection capacity. The coating does not peel or crack upon bending and is electrochemically stable. Finally, we demonstrated the use of the coated microfiber electrodes for localized neural stimulation and high-resolution neural recording. Although CNWs have been used in applications such as field emission devices[11], fuel cells[12], batteries[13] and supercapacitors[14] due to their large

surface areas, to our knowledge, this is the first report of CNW coated carbon fibers for neural interfacing.

2. Results and Discussion

2.1. B-CNW Deposition

2.1.1. Surface morphology

Deposition of B-CNW was performed using microwave plasma enhanced chemical vapor deposition (CVD), with a gas mixture of trimethyl boron (TMB), CH_4 and H_2. Prior to deposition, CFs were functionalized with nanodiamonds, as previously described[9]. The functionalized CF bundles were sandwiched between two molybdenum blocks, with the tips located within a 3d printed titanium cage (**Figure 1a**). The cage improved the plasma distribution on the fibers, leading to a more uniform B-CNW growth on the CFs (**Figure S1**). B-CNW showed maze-like vertical structures on the CF surfaces (Figure 1b). The coverage and thickness of the coating varied according to the deposition time (**Figure S2**). At least 2 h of deposition was required for a uniform B-CNW coating and the coated fiber diameter increased from the 7 µm of the uncoated CFs up to 30 µm after 6 h of deposition (Figure S2). In the following work, we used 2 h of deposition, which resulted in a coated fiber diameter of approximately 10 µm.

2.1.2. Flexibility

The flexibility of CFs was retained after coating, as illustrated in Figure 1c. The fibers could be bent easily without any visible cracks or delamination of the coating under SEM imaging. We also

compared the flexibility of the B-CNW coated fibers with our previously reported N-UNCD coated CFs (**Figure S3**). However, the N-UNCD coated fibers showed cracks and delamination during the bending studies.

2.1.3. Boron doping

The presence of boron in the coating was expected due to the gas mixture used during CVD, and was confirmed by X-ray photoelectron spectroscopy (XPS). In addition to the C1s and O1s peaks, a small B1s peak was detectable from the survey spectrum (Figure 1di). Fitting of the high resolution B1s spectrum indicates the presence of different forms of C-B bands (Figure 1dii). From the fitting of the high resolution C1s spectrum, we found that the B-CNW coating exhibited a C-B band at a peak position of 282.3 eV[15] (Figure 1diii), which contributed to about 1% of the carbon bonding. The comparison of the high-resolution C1s spectra obtained from the bare CFs and the B-CNW CFs with different deposition times is summarized in **Figure S4**. Furthermore, the presence of boron in the B-CNW surfaces was confirmed using a Raman spectrometer (**Figure S5**). Near Edge X-ray Absorption Fine Structure (NEXAFS) measurements, as shown in **Figure S6**, indicate that the B-CNW surfaces were sp^2 bonded carbon dominant, without much evidence of sp^3 bonded carbon.

2.1.4. Cytotoxicity

There have been concerns about the cytotoxicity of boron inclusion in materials[16]. Therefore, we studied the potential use of the B-CNW coated fibers for supporting neuron growth. Figure 1e shows an example area of primary rat cortical neurons on the B-CNW coated fibers after 7 days of culturing. The neurons survived well and proliferated on the samples and neurites could adhere and grow along

the fiber surfaces (Figure 1eiii). Combining their small diameter, flexibility and capacity for supporting neuron growth, these fibers are expected to minimize the chronic inflammation and neuronal loss during long-term implantation.

2.2. Electrochemical Characterization

2.2.1. Electrochemical properties

The microelectrodes were fabricated using both the coated and uncoated CFs for electrochemical measurements, neural stimulation and recording (**Figure 2a**). The fabrication procedures were the same as previously described[9]. Briefly, individual fibers were first attached onto copper wires via silver epoxy, and then encapsulated in the glass capillaries pulled using a micropipette puller. The lengths of the fibers exposed were controlled to be 100 ± 10 μm. Finally, an electrical connection was made from the other end of the copper wires. As the uncoated and coated CFs have diameters of 7 μm and 10 μm, the geometric surface areas (GSAs) of the electrodes are 2238 ± 220 μm^2 and 3220 ± 314 μm^2, respectively.

We found that the B-CNW coating significantly boosted the electrochemical properties of the electrodes. The most relevant electrochemical properties for neural stimulation and recording are the charge injection capacity (CIC) and the electrochemical impedance. CIC describes the maximum charge that can be safely injected into an electrode before water splitting occurs. The water windows for both CF and B-CNW electrodes were measured by cyclic voltammetry (CV) in PBS (Figure 2b). The water window increased from -0.4 V ~ 0.6 V on CFs to -1.8 V ~ 1.2 V on B-CNW coated electrodes. For CIC calculations, biphasic current pulses with phase duration of 500 μs was injected

into the electrodes and we measured the potential transient responses from the electrodes (**Figure S7**). After B-CNW coating, CIC increased more than 330 times from the values measured from uncoated fibers, i.e. from 0.024 ± 0.008 mC cm^{-2} to 7.82 ± 0.35 mC cm^{-2} (Figure 2c). Similar measurements were performed on the coated electrodes with other fiber lengths (10 μm and 50 μm), but no statistically significant difference was observed for the different exposed fiber lengths. (Figure S7). This CIC value is comparable to other previously reported high-capacitance coating materials and is significantly larger than conventional metal based electrodes (TiN and Pt) (**Table 1**). The electrochemical impedance at 1 kHz is another commonly used value for evaluating electrodes. Higher impedance will consume more power for neural stimulation and lead to a higher noise level during recording. Therefore lower electrode/tissue impedance is desired for neural interfacing. From electrochemical impedance spectroscopy (EIS) measurements, we found a drop of impedance following B-CNW coating at the full frequency range of the measurement, between 1 Hz and 10^5 Hz (Figure 2d-e). The impedance at 1kHz dropped from 130 kΩ down to about 30 kΩ (Figure 2f, Table 1). However, further research is required to determine whether the improvement of electrochemical properties is merely due to the larger surface area of CNWs, or also a result of boron doping.

2.2.2. Electrochemical stability

The ability of the electrode to maintain its properties is essential for long-term neural interfaces. Therefore, we also evaluated the electrochemical stability of the B-CNW coated electrodes following long-term electrical stimulation. The first test was performed by applying repeated CVs on the electrode over a potential range of 0-1V (**Figure 3a**). This positive potential range is within the electrode water window. By repeatedly charging the electrode, we studied the adherence of B-CNW coating on the electrode surface. The surface morphology of the same B-CNW electrode before and

after 1000 CV cycles was characterized using SEM. As shown in Figure 3b, there was no noticeable change and the coating clearly did not peel off from the CF surfaces. Using EIS, we measured the impedance of the electrode at 1 kHz after different numbers of CV cycles. The impedance also remained stable and significantly lower than the uncoated CF electrodes (Figure 3c). In addition to the repeated CVs, another stability test was performed by applying electrical pulses on the electrodes. Here we used biphasic pulses with phase duration of 0.1 ms at a current amplitude of 500 μA. Such parameters were chosen as they were found effective for stimulating retinal ganglion cells (RGCs), as shown in **Figure 4**. The change of CIC following the pulsing test was monitored over time using voltage transient measurements. As shown in Figure 3d, although there was a small fluctuation of CIC after different pulses, the value remained above 7 mC cm^{-2} even after 500,000 repeats, which is much larger than that of the CF electrodes (0.02 mC cm^{-2}).

2.3. Neural stimulation and recording

2.3.1. In vitro neural stimulation

Having demonstrated the promising electrochemical properties of the coated CF electrodes, we now report their performance when used for neural stimulation and recording. The stimulation was performed using explanted rat retina (**Figure 4**). Axon bundle stimulation has been found to limit the resolution of vision restored by retinal prostheses. Unwanted axon bundle activation leads to retinal ganglion cells (RGCs) being activated far away from the stimulating electrodes, forming an elongated activation pattern. One strategy to avoid axon bundle stimulation requires the use of long, narrow rectangular electrodes (10 μm wide and >100 μm long) placed parallel to axon bundles[17]. However, microwire electrodes with such geometry, fabricated with electrode materials commonly used in retinal prosthesis development, such as platinum,[18] normally do not have a CIC large enough for

neural stimulation. In this work, we tested the strategy for localized RGC stimulation using B-CNW coated CF electrodes (10 μm in diameter, 100 μm long). By loading calcium indicators (OGB-1) into the wholemount retina from Long Evans rats, we have previously developed a technique to image the spatial distribution of RGC responses to stimulation[19]. Here, the electrodes were placed with an angle of 15° to the retinal surface, either parallel with or perpendicular to the direction of the axon bundles. As the full exposed fiber was in contact with the perfusion, the full length was involved in the stimulation. As shown in Figure 4a and 4b, when the electrodes were parallel with the axon bundles, the electrodes mainly stimulated nearby RGCs. The charge required for stimulation could exceed 1.55 mC cm^{-2}, higher than the CIC limits of many conventional electrode materials (Table 1). However, when using the same stimulation parameters, the electrodes perpendicular to the axon bundles led to RGC activation spread along the direction of the axon bundles (Figure 4c, 4d). These results are consistent with previous simulation results[17]. A more detailed discussion about the effect of different electrode configurations on the RGC activation pattern has been reported elsewhere[20]. Using such electrodes, we were able to stimulate RGCs with high spatial selectivity.

2.3.2. In vivo Neural Recording

Finally, we demonstrated the capability of B-CNW electrodes for high quality *in vivo* single-unit neural recording (**Figure 5**), similar to our previous reports[9]. The electrodes were inserted into layer 4/5 of the visual cortex of an Australian marsupial (Tamar Wallaby, Macropus Eugenii) as part of ongoing comparative investigations. The extracellular signals were sampled at 30 kHz with a 14.5 kHz lowpass filter. For postprocessing, the raw data was filtered using a bandpass of 500 and 14250 Hz. The electrodes produced clear action potentials that could be readily extracted from the background noise, using spike-sorting algorithms. We were able to isolate 1-2 single units per electrode, and one

example is shown in Figure 5a and 5b. To make sure that the potentials were unequivocally from visual neurons, we used moving grating patterns on an LCD display to activate the visual neurons in V1. Figure 5c shows the response of the recorded neuron to grating patterns with different orientations. The neuron was most sensitive to an orientation of -22.5°. Figure 5d shows a raster plot generated by moving gratings with a range of orientations through the receptive fields of V1 neurons. The moving stimulus started at time 0 and finished at time 1 s. The synchronized firing of spikes at –0.5 s and 1.5 s is due to the static grating turning on and off, respectively (i.e. the stimulus is on from -0.5 s to 1.5 s, but is only moving from 0 s to 1 s). Around 0.1 s after stimulus onset there was a clear increase in spike rate, which dropped off approximately 0.1 s after stimulus offset. The timing of the response is clearly revealed by the peristimulus time histogram (Figure. 5e). The SNR was determined according to the formula:

$$SNR = S_{-pp} / 2\sigma_{Noise} \quad (2)$$

where S_{-pp} is the mean peak-to-peak spike amplitude, and σ_{Noise} is the standard deviation after all the identified spike waveforms had been removed. In this recording, SNR was 6.7. This value is comparable to other *in vivo* recording electrodes according to the same SNR definition, such as PEDOT/carbon nanotube (3 ± 0.6)[21] and N-UNCD coated CF electrodes (3.8)[9].

2.4. Discussion

This work shows that B-CNW coatings improve the performance of CF microelectrodes. As compared to planar electrodes, these microfiber electrodes are cylindrical, narrow and flexible. They have smaller dimensions and therefore cause less damage and tissue displacement following

implantation, and are potentially more suitable for chronic applications[22]. While most coating technologies have been designed to increase the surface area of planar electrode arrays, the B-CNW coating reported in this work is applicable for ultrathin microfibers. As summarized in Table 1, the electrochemical properties of the B-CNW coated electrodes are comparable to many other high surface area materials.

Previous research indicated that CIC is dependent on both the electrode GSA and pulse duration used in the voltage transient measurement[4, 6b, 23]. In this study, the CIC measurements were conducted using 500 μs pulses, a commonly used duration in many other reports[9, 24]. As CIC increases with pulse duration, the CIC of B-CNW coated fibers is smaller than that of PEDOT:PSS -co-MA coated CFs, but larger than that of iridium oxide coated CFs without bias, and 2 orders of magnitude larger than that of the uncoated CFs. We performed most of the experiments with an electrode fiber length of 100 μm, which is required for avoiding RGC axon bundle activation and for creating localized neural responses in the explanted retina (Section 2.3.1). Although the resulting GSA (3220 μm^2) is larger than that used in some studies in Table 1, we found that the CIC value remains the same (within statistical error) even when the exposed electrode length is reduced from 100 to 10 μm, (Figure S7) . This is consistent with another study[23a], in which the authors reported similar CIC values for microelectrodes with diameters between 20 and 150 μm (GSA: 314 – 17 671 μm^2).

For potential long-term chronic applications, the stability of the coating is essential. The B-CNW coating adheres well to CF surfaces, with no delamination or cracking upon bending. In comparison, our previously reported N-UNCD coating provides promising electrochemical properties, but the coating delaminates when the electrodes are bent. In this work, we demonstrate the stability of B-CNW coating after repetitive electrical stimulation in saline solution. After 1000 CV cycles and 500,000 repetitive biphasic pulses, we show that the electrodes retained their CIC and impedance, and there was no substantial change observed from SEM on the coating morphology. PEDOT based polymers and iridium oxide are another two types of coating reported for carbon fibers. The electrochemical properties of PEDOT coatings have been shown to degrade in saline within the same number of CV cycles [25] and iridium oxide coatings were found to delaminate following continuous over pulsing[26].

Compared to conductive polymers and iridium oxide, B-CNW coated CFs with only 1% of boron doping provides a completely carbon-based solution. They can support neuron adhesion and neurite outgrowth, and are expected to be safer for implantation. However, it is unknown if the properties of B-CNW coating will change chronically after implantation due to possible biofouling and microglia formation. Future work will focus on the assessment of their performance and stability in long-term chronic studies. In this work, we used glass for fiber insulation for convenience to control the exposed fiber length for accurate surface area measurement and to meet the requirement for avoiding RGC axon bundle activation. However, the use of glass insulation may hinder its chronic application. Polymer coatings, such as Parylene-C, will be used to replace glass insulation in the chronic work.

3. Conclusion

We report a new type of coating, boron doped carbon nanowalls (B-CNW), on carbon fiber (CF) microelectrodes for high-resolution neural stimulation and recording. The coating significantly improved the electrochemical properties of CF microelectrodes, reaching a charge injection capacity of 7.82 ± 0.35 mC cm^{-2}. We demonstrated the flexibility, biocompatibility and stability of the B-CNW coating. These electrodes successfully delivered localized stimulation in the explanted retina, while recording single-units from the visual cortex with signal to noise ratio as high as 6.7. The B-CNW coated CFs are expected to improve the overall performance of neural interfaces for long-term applications.

4. Experimental Section

B-CNW Deposition: PAN-based Carbon Fibers (CF, Goodfellow) were first functionalized with nanodiamonds, as described previously[9]. Briefly, the CFs were first functionalized with nitrophenyl groups, and then aminophenyl groups via two-step electrochemistry. Following aminophenyl functionalization, they were covalently seeded with oxygen-terminated nanodiamond via EDC chemistry. After nanodiamond seeding, the CFs were placed in a microwave plasma-assisted chemical vapor deposition (CVD) system for boron-doped carbon nanowall (B-CNW) growth. The fibers were held in place by two molybdenum blocks, and approximately 1 cm of each fiber tip was placed in a 3D printed titanium cage. The titanium cage improved the distribution of plasma across the fibers and led to uniform growth of B-CNW. During B-CNW deposition, a gas mixture of 87% H_2,

4% CH_4 and 9% trimethyleboron (TMB) was used at a pressure of 40 torr and a power of 1500 W. The deposition time was varied between 1 and 6 h.

Single-fiber Electrode Fabrication: For electrochemical measurements and neural stimulation and recording, 2 h B-CNW coated fibers were used. Single fiber microelectrodes were fabricated using uncoated CFs and B-CNW coated fibers, as previously described[1]. Briefly, single fibers were first attached onto copper wires via silver epoxy, and then insulated in pulled glass capillaries. The exposed fiber lengths were adjusted to 100 ± 10 µm. An electrical connection was made from the other end of the copper wires with silver epoxy.

Surface Characterization: The morphology of the fibers after each time interval of B-CNW deposition was obtained with SEM/FIB Nova 200 Nanolab, FEG Dual Beam (HV 5 KV, Current 6.3 nA, mode SE). X-Ray Photoelectron Spectroscopy (XPS) data were collected in a Thermo-Fisher K-Alpha apparatus (10^{-9} mbar) using an Mg Ka radiation source at a power of 300 W. The spot size was 400 mm and survey spectra were measured at a 200 eV pass energy. Raman spectra were taken on both CFs and B-CNW coated fibers using a Renishaw inVia Raman Spectrometer with a laser excitation of 532 nm and power of 100 mW at room temperature. K-edge NEXAFS measurements were conducted in the Soft X-Ray beamline of the Australian Synchrotron. All measurements were conducted in the total electron yield mode, recorded using sample drain current to collect a signal of all secondary electrons and thus data from the bulk of the samples. Double normalization was conducted with an 'IO' gold grid partially inserted into the beam, to monitor fluctuations in beam intensity for all scans,

and normalized to a reference photodiode scan for beamline transmission function (primarily for removal of beamline carbon-based absorption characteristics)[27] .

Electrochemical Characterization: For electrochemical characterization, cyclic voltammetry (CV) and electrical impedance spectroscopy (EIS) measurements were performed using a potentiostat (Gamry, Interface 1000E). All voltammograms were obtained with the electrodes immersed within a Teflon electrochemical cell of three electrodes, where platinum and Ag/AgCl are counter and reference electrodes, respectively. All experiments were conducted in 1 M PBS (0.13 M NaCl) at room temperature without nitrogen gas bubbling. Charge injection capacity (CIC) was measured from voltage transients during a constant current stimulation pulse (0.5 ms biphasic pulses) as described previously,[9] according to the method of Cogan *et al*.[4], using a Tucker Davis Technologies system (RZ2 base station and IZ2 multichannel stimulator).

Stability Test: Two different stability tests were performed. The first stability test was conducted by applying 1000 repeated CVs to the B-CNW coated microelectrodes within a potential range of 0 - 1V, at a scan rate of 100 mV s^{-1} in 1 M PBS. The electrochemical properties of the electrodes were characterized after every 100 CVs using EIS. In the second stability test, biphasic stimulation with phase duration of 0.1 ms, current amplitude of 500 µA, was applied on the electrodes. A total of 500 k pulses were used and the CIC was measured using voltage transient measurements after every 100 k pulses.

Cytotoxicity Evaluation: All experimental procedures conformed to the policies of the National Health and Medical Research Council of Australia (NHMRC) and were approved by the Animal Experimental Ethics Committee of the University of Melbourne (Ethics Approval # 1814396). The B-CNW coated CF bundles were secured on coverslips using Polydimethylsiloxane (PDMS), with most of the fiber surface exposed. The fibers were sterilized using an autoclave, placed in a 24-well dish and then coated with 0.05 mg ml^{-1} poly-d-lysine (Sigma). Primary rat cortical cultures were obtained by isolating the cerebral cortices from one-day-old rats, as previously described[28]. Briefly, the heads were removed and placed in Hank's balanced salt solution (HBSS; Gibco). Then the skin and top of the skull were removed and a small area of cortex was pinched off with fine forceps. Meninges were removed and the tissue was chopped with a scalpel blade. The tissue was dissociated by protease digestion for 20 min at 37 °C using 10 µg ml^{-1} DNAse 1 (Sigma) and 250 µg ml^{-1} trypsin (Sigma) in HBSS. Trypsinisation was terminated by using Soybean Trypsin Inhibitor (Sigma) containing 10µg ml^{-1} DNAse 1 and the cells were pelleted by centrifuging and triturated using a P1000 pipette. The cells were diluted in culture medium (Neurobasal A with 2% B27 supplement, 2 mM Glutamax, 100 µg ml^{-1} penicillin, 100 µg ml^{-1} streptomycin, and 5% fetal calf serum). Finally, the cells were seeded on B-CNW coated CF surfaces at a density of 40,000 cells per well. The cell cultures were incubated at 37°C in 5% CO_2. Half of the culture medium was replaced at Day 4.

After 7 days of incubation, the samples were washed with PBS once and fixed in 4% paraformaldehyde in PBS for 10 min at room temperature, followed by cold (-20 °C) methanol for another 10 min. After washing with PBS three times, the samples were incubated in a blocking

solution (2% fetal calf serum and 2% normal goat serum in PBS) for 30 min. The samples were then incubated for 20 min with primary antibody (mouse anti-beta-III tubulin) at room temperature. Following PBS wash, the samples were incubated with secondary antibody (Alexa 488-conjugated goat anti-mouse immunoglobulin). They were finally washed with PBS and imaged using a confocal microscope (Olympus, FV 1200). Images were obtained using an excitation laser at 473 nm, through a Nikon Plan Apo 0.75-numerical aperture (NA) x40 objective.

Ex vivo Neural Stimulation: All experimental procedures conformed to the policies of the National Health and Medical Research Council of Australia (NHMRC) and were approved by the Animal Experimental Ethics Committee of the University of Melbourne (Ethics Approval # 1814462). Neural stimulation was performed using Long-Evans rats older than 3 months, of either gender, as previously described[9]. Briefly, the animals were anesthetized prior to enucleation, and then sacrificed with an overdose of Letharbarb. The calcium indicators (20 mM OGB-1) were injected into each eye through the optic nerve. After removing the cornea and lens, the retina was left overnight at room temperature in a dish filled with carbogenated Ames medium. On the second day, one piece of retina was mounted with retinal ganglion cell (RGC) side up, held in a perfusion dish, and imaged under a confocal microscope (Olympus, FV 1200). During the experiment, the retina was perfused with heated carbogenated Ames medium (33-35 °C) at a rate of 4-6 ml min^{-1}.

To deliver electrical stimulation, the B-CNW coated electrodes were placed at an angle of 15° with the retinal surfaces. The tips were in contact with the retinal surfaces. The electrodes were either

parallel with or perpendicular to the axon bundles. Images were obtained using an excitation laser at 473 nm, through a Nikon Plan Apo 0.75-numerical aperture (NA) x20 objective. Stimuli were delivered using a Ripple system and images were acquired at 7.8 Hz and synchronized to the onset of each stimulus. Each stimulus was composed of ten anodic first biphasic pulses at a frequency of 60 Hz, with pulse duration of 0.1 ms. Data processing was performed in Fiji (ImageJ) and MATLAB R2018b.

In vivo Neural Recording: All experimental procedures conformed to the policies of the National Health and Medical Research Council of Australia (NHMRC) and were approved by the Animal Experimental Ethics Committee of the University of Melbourne (Ethics Approval # 1714178). *In vivo* recording was obtained from the primary visual cortex of a Tammar Wallaby (*Macropus Egenii*), as previously described[9]. The electrode testing was conducted as a part of ongoing comparative neuroscience projects and was performed at the conclusion of a long-term acute experiment. Briefly, the animal was anesthetized, intubated and then connected to a ventilator and aesthesia machine. The health of the animal was monitored throughout the entire experiment by checking the electrocardiogram (ECG), electroencephalogram (EEG), respiration rate, blood pressure, end-tidal CO_2 concentration and oxygen concentration. The head of the wallaby was stabilized with a stereotaxic frame and custom-made ear bars. A craniotomy was conducted to access the primary visual cortex (V1) in the left hemisphere. Electrodes were implanted 1200 µm deep for recording. Therefore, the recording is likely to be collected from the lower strata of layer 4/5.

Visual stimuli were generated with a ViSaGe visual stimulus generator (Cambridge Research Systems, Carmbridge UK) and displayed on a calibrated LED monitor. The monitor was viewed monocularly from 30 cm distance. During single-unit recording, drifting sinusoidal gratings at varying orientations (0° to 337.5° in 22.5° increments at 5 trials each orientation) were presented to determine the preferred orientation of the recorded neurons. The extracellular signals were sampled at 30 kHz with a 14.5 kHz lowpass filter. For postprocessing, the raw data was filtered using a bandpass of 500 and 14,250 Hz. Multi-unit activity (MUA) was recorded, and the signals were amplified and filtered. Signals were automatically sorted through KiloSort[29], then manually curated using phy[30] to sort single units from MUA. After spike-sorting, single units could be readily identified.

The signal quality was defined according to the signal to noise ratio (SNR), which was calculated as the peak-to-peak amplitude of the mean waveform of the cluster divided by twice the standard deviation of the noise[21], as shown in formula (2).

Supporting Information

Supporting Information is available from the Wiley Online Library or from the author.

Acknowledgements

This research was funded by a Project Grant from The National Health and Medical Research Council of Australia (GNT1101717). The authors acknowledge use of the Advanced Microscopy Facility at Bio21 (The University of Melbourne) for SEM imaging and the National Vision Research Institute for use of electrophysiology equipment. The authors also acknowledge the facilities, and the scientific and technical assistance of the RMIT Microscopy & Microanalysis Facility (RMMF), a linked

laboratory of Microscopy Australia, and the RMIT Advanced Manufacturing Precinct. The work was performed in part at the Melbourne Center for Nanofabrication (MCN) in the Victorian Node of the Australian National Fabrication Facility (ANFF). WT is supported by a Medical/Science Grant from the CASS Foundation (Ref 8612). DJG is supported by an ANFF/MCN Technology Ambassador Fellowship. AN is supported by the Australian Research Council via Linkage Grant LP160101515. SP is a shareholder of iBIONICS, a company developing a diamond based retinal implant. SP and DJG are shareholders and public officers of Carbon Cybernetics Pty Ltd, a company developing diamond and carbon-based medical device components. The other authors declare no conflict of interest.

Received: ((will be filled in by the editorial staff))
Revised: ((will be filled in by the editorial staff))
Published online: ((will be filled in by the editorial staff))

References

[1] a) Y. Zhang, J. Ding, B. Qi, W. Tao, J. Wang, C. Zhao, H. Peng, J. Shi, *Advanced Functional Materials* **2019**; b) G. Hong, C. M. Lieber, *Nature Reviews Neuroscience* **2019**, 20, 330.

[2] a) K. Wang, C. L. Frewin, D. Esrafilzadeh, C. Yu, C. Wang, J. J. Pancrazio, M. Romero-Ortega, R. Jalili, G. Wallace, *Adv Mater* **2019**, 31, 1805867; b) D. Y. Lewitus, J. Landers, J. R. Branch, K. L. Smith, G. Callegari, J. Kohn, A. V. Neimark, *Advanced Functional Materials* **2011**, 21, 2624; c) T. D. Y. Kozai, N. B. Langhals, P. R. Patel, X. P. Deng, H. N. Zhang, K. L. Smith, J. Lahann, N. A. Kotov, D. R. Kipke, *Nat Mater* **2012**, 11, 1065; d) F. Vitale, S. R. Summerson, B. Aazhang, C. Kemere, M. Pasquali, *Acs Nano* **2015**, 9, 4465; e) H. Vara, J. E. Collazos-Castro, *Acta Biomaterialia* **2019**, 90, 71; f) H. Vara, J. E. Collazos-Castro, *Acs Appl Mater Inter* **2015**, 7, 27016.

[3] V. Viswam, M. E. J. Obien, F. Franke, U. Frey, A. Hierlemann, *Front Neurosci-Switz* **2019**, 13, 385.

[4] S. F. Cogan, *Annu. Rev. Biomed. Eng.* **2008**, 10, 275.

[5] S. M. Won, E. Song, J. Zhao, J. Li, J. Rivnay, J. A. Rogers, *Adv Mater* **2018**, 30, 1800534.

[6] a) P. R. Patel, H. N. Zhang, M. T. Robbins, J. B. Nofar, S. P. Marshall, M. J. Kobylarek, T. D. Y. Kozai, N. A. Kotov, C. A. Chestek, *J Neural Eng* **2016**, 13; b) F. Deku, A. Joshi-Imre, A. Mertiri, T. J. Gardner, S. F. Cogan, *J Electrochem Soc* **2018**, 165, D375; c) C. L. Kolarcik, K. Catt, E. Rost, I. N. Albrecht, D. Bourbeau, Z. H. Du, T. D. Y. Kozai, X. L. Luo, D. J. Weber, X. T. Cui, *J Neural Eng* **2015**, 12.

[7] M. L. Huffman, B. J. Venton, *Analyst* **2009**, 134, 18.

[8] M. K. Zachek, A. Hermans, R. M. Wightman, G. S. McCarty, *J Electroanal Chem* **2008**, 614, 113.

[9] M. A. Hejazi, W. Tong, A. Stacey, A. Soto-Breceda, M. R. Ibbotson, M. Yunzab, M. I. Maturana, A. Almasi, Y. J. Jung, S. Sun, *Biomaterials* **2019**, 119648.

[10] Y. H. Wu, P. W. Qiao, T. C. Chong, Z. X. Shen, *Adv Mater* **2002**, 14, 64.

[11] E. Stratakis, R. Giorgi, M. Barberoglou, T. Dikonimos, E. Salernitano, N. Lisi, E. Kymakis, *Appl Phys Lett* **2010**, 96.

[12] S. C. Shin, A. Yoshimura, T. Matsuo, M. Mori, M. Tanimura, A. Ishihara, K. Ota, M. Tachibana, *J Appl Phys* **2011**, 110.

[13] Z. Gonzalez, S. Vizireanu, G. Dinescu, C. Blanco, R. Santamaria, *Nano Energy* **2012**, 1, 833.

[14] T. C. Hung, C. F. Chen, W. T. Whang, *Electrochem Solid St* **2009**, 12, K41.

[15] K. Siuzdak, M. Ficek, M. Sobaszek, J. Ryl, M. Gnyba, P. Niedzialkowski, N. Malinowska, J. Karczewski, R. Bogdanowicz, *Acs Appl Mater Inter* **2017**, 9, 12982.

[16] D. J. Garrett, A. L. Saunders, C. McGowan, J. Specks, K. Ganesan, H. Meffin, R. A. Williams, D. A. Nayagam, *Journal of Biomedical Materials Research Part B: Applied Biomaterials* **2016**, 104, 19.

[17] F. Rattay, S. Resatz, *IEEE transactions on biomedical engineering* **2004**, 51, 1659.

[18] J. D. Weiland, S. T. Walston, M. S. Humayun, *Annu Rev Vis Sci* **2016**, 2, 273.

[19] W. Tong, M. Stamp, N. V. Apollo, K. Ganesan, H. Meffin, S. Prawer, D. J. Garrett, M. R. Ibbotson, *J Neural Eng* **2019**, 17, 016018.

[20] W. Tong, M. Hejazi, D. J. Garrett, T. Esler, S. Prawer, H. Meffin, M. Ibbotson, *J Neural Eng* **2020**.

[21] T. D. Y. Kozai, K. Catt, Z. H. Du, K. Na, O. Srivannavit, R. U. M. Haque, J. Seymour, K. D. Wise, E. Yoon, X. T. Cui, *Ieee Transactions on Biomedical Engineering* **2016**, 63, 111.

[22] K. M. Szostak, L. Grand, T. G. Constandinou, *Front Neurosci-Switz* **2017**, 11, 665.

[23] a) M. Ganji, A. Tanaka, V. Gilja, E. Halgren, S. A. Dayeh, *Advanced Functional Materials* **2017**, 27, 1703019; b) J. D. Weiland, D. J. Anderson, M. S. Humayun, *IEEE transactions on biomedical engineering* **2002**, 49, 1574.

[24] N. V. Apollo, M. I. Maturana, W. Tong, D. A. X. Nayagam, M. N. Shivdasani, J. Foroughi, G. G. Wallace, S. Prawer, M. R. Ibbotson, D. J. Garrett, *Advanced Functional Materials* **2015**, 25, 3551.

[25] a) C. Boehler, F. Oberueber, T. Stieglitz, M. Asplund, presented at 2015 7th International IEEE/EMBS Conference on Neural Engineering (NER) **2015**; b) R. A. Green, L. A. Poole-Warren, N. H. Lovell, presented at 2007 3rd International IEEE/EMBS Conference on Neural Engineering **2007**.

[26] a) S. F. Cogan, A. A. Guzelian, W. F. Agnew, T. G. Yuen, D. B. McCreery, *J Neurosci Meth* **2004**, 137, 141; b) S. J. Wilks, S. M. Richardson-Burn, J. L. Hendricks, D. Martin, K. J. Otto, *Frontiers in neuroengineering* **2009**, 2, 7.

[27] A. Stacey, N. Dontschuk, J. P. Chou, D. A. Broadway, A. K. Schenk, M. J. Sear, J. P. Tetienne, A. Hoffman, S. Prawer, C. I. Pakes, *Advanced Materials Interfaces* **2019**, 6, 1801449.

[28] W. Tong, K. Fox, A. Zamani, A. M. Turnley, K. Ganesan, A. Ahnood, R. Cicione, H. Meffin, S. Prawer, A. Stacey, D. J. Garrett, *Biomaterials* **2016**, 104, 32.

[29] M. Pachitariu, N. Steinmetz, S. Kadir, M. Carandini, K. D. Harris, *BioRxiv* **2016**, 061481.

[30] C. Rossant, S. N. Kadir, D. F. Goodman, J. Schulman, M. L. Hunter, A. B. Saleem, A. Grosmark, M. Belluscio, G. H. Denfield, A. S. Ecker, *Nature neuroscience* **2016**, 19, 634.

[31] Y. Lu, T. Li, X. Zhao, M. Li, Y. Cao, H. Yang, Y. Y. Duan, *Biomaterials* **2010**, 31, 5169.

[32] K. Wang, H. A. Fishman, H. J. Dai, J. S. Harris, *Nano Lett* **2006**, 6, 2043.

[33] S. Venkatraman, J. Hendricks, Z. A. King, A. J. Sereno, S. Richardson-Burns, D. Martin, J. M. Carmena, *IEEE transactions on neural systems and rehabilitation engineering* **2011**, 19, 307.

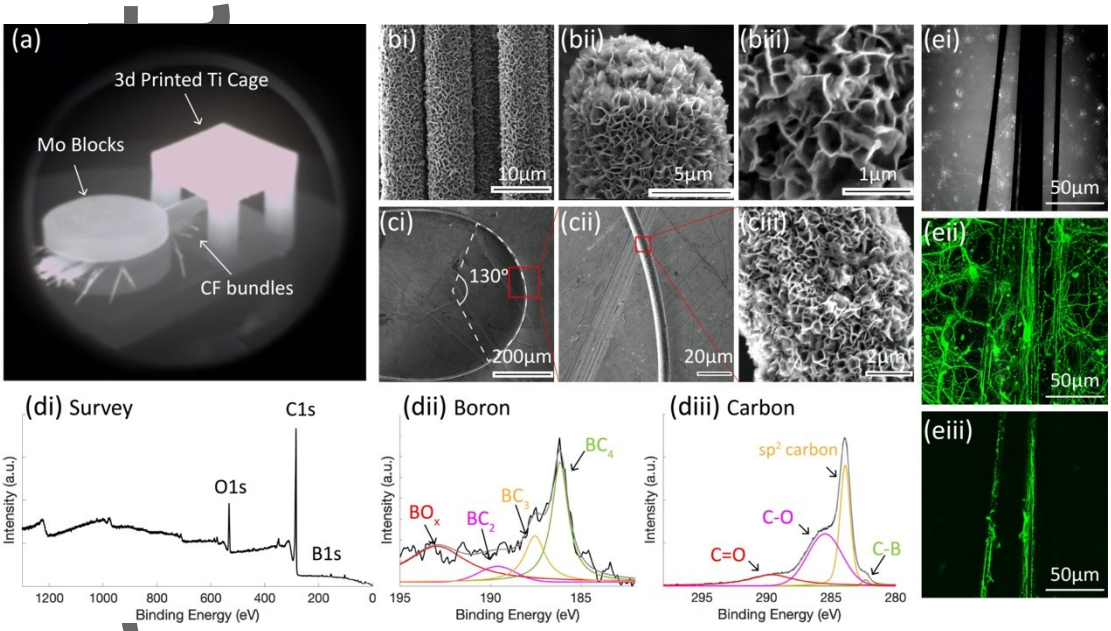

Figure 1. B-CNW was deposited as a coating on the CF surfaces. (a) B-CNW were deposited on CFs using microwave plasma-assisted chemical vapor deposition. During deposition, the CFs were secured in two molybdenum blocks, with the tips in a 3d printed titanium cage for uniform B-CNW growth. (b) B-CNW coating after 2 h of deposition was imaged with an SEM under different magnifications. The coatings on the surface show maze-like vertical structures on the CF surfaces and the fiber diameter after coating was about 10 µm. (c) B-CNW coating did not change the flexibility of CFs and coated fibers could be bent easily. One example fiber is shown in Figure ci and no delamination was found after bending (cii&ciii). The bending angle and radius are indicated in Figure ci. (d) XPS was performed to study the surface chemical structures of the coated fibers. The survey spectrum (di) shows a small peak representing boron on the surfaces. The high-resolution B1s spectrum (dii) can be fitted with four different carbon boron bands, including BC_4 at 186.1 eV, BC_3 at 187.3 eV, BC_2 at 189.6 eV and BO_x at 193.0 eV. The high resolution C1s spectrum (diii) can be fitted with C-B band at 282.4 eV, sp2 carbon band at 284 eV, C-O band at 285.6 eV and C=O band at 290 eV. (e) primary rat cortical neurons could survive and proliferate on B-CNW coated CFs (2 h deposition) after 7 days of incubation. (ei) phase contrast image. (eii) depth profile of ß-III tubulin staining (eiii) ß-III tubulin staining on the fiber surface.

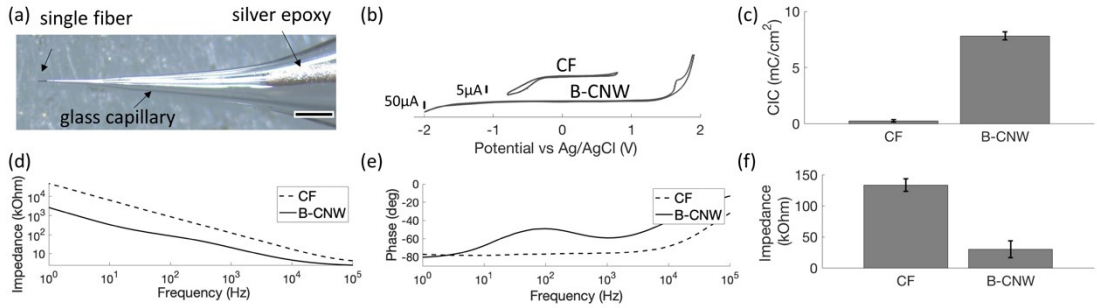

Figure 2. B-CNW coated electrodes exhibited improved electrochemical properties. (a) Optical image of the microelectrodes fabricated for electrochemical measurements. Single fibers were attached to copper wires using silver epoxy and then insulated in pulled glass capillaries. The lengths of the fibers exposed were controlled to be about 100 µm. The same microelectrodes were used for stability testing in Figure 3, neural stimulation in Figure 4 and recording in Figure 5. Scale bar: 100 µm. (b) Water windows of CF and B-CNW, measured using CV at a scan rate of 100 mV s^{-1} in PBS. (c) Charge injection capacity (CIC) measured for both CF and B-CNW coated electrodes. Error bar indicates the standard deviation, n=3. (d, e) Modulus and phase angle of impedance of electrodes, respectively. (f) Impedance at 1kHz measured using EIS. Error bars indicate the standard deviation, n=3.

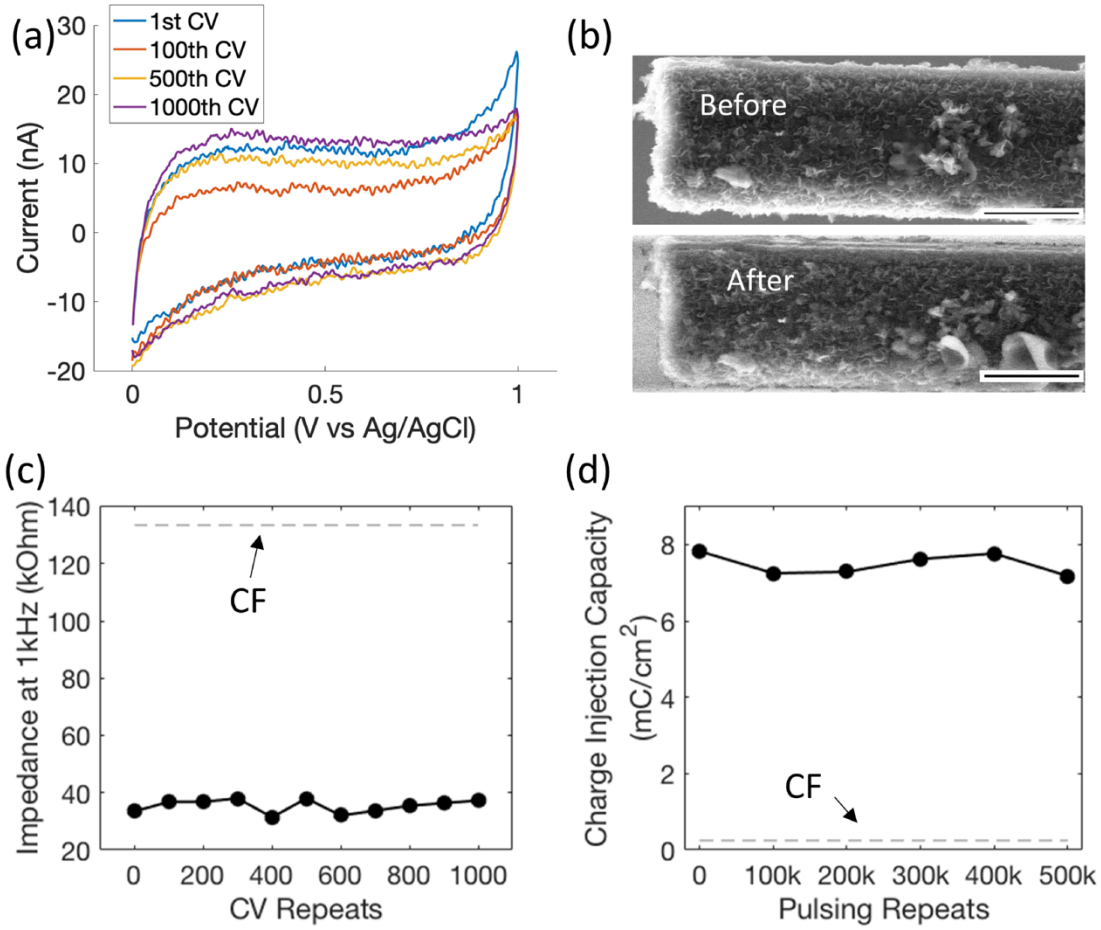

Figure 3. B-CNW coated electrodes were electrochemically stable. (a) Prolonged CVs of the B-CNW coated electrodes, 1000 cycles within a potential range between 0 and 1 V at a scan rate of 100 mV s^{-1} in PBS at a scan rate of 100 mV s^{-1} in PBS. (b) SEM images of the same B-CNW coated electrode tip before and after CV stability test. Scale bar: 10 µm. (c) The impedance at 1kHz measured by EIS for B-CNW electrodes (solid line) during the repeated CVs remained significantly lower than that of CF electrodes (dash line). (d) CIC of B-CNW electrodes (solid line) remained above 7 mC cm^{-2} after repeated biphasic stimulation (0.1ms, 500 µA), and much larger than CIC of CF electrodes.

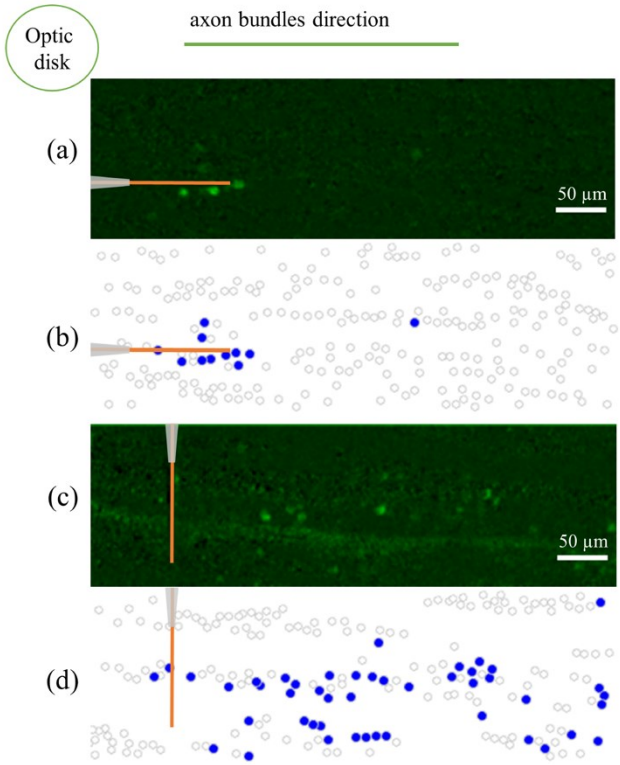

Figure 4. B-CNW coated CF electrodes could elicit localized responses from RGCs in explanted rat retinas. (a) and (c) show the background subtracted calcium imaging of the RGC response. The neurons activated are labelled blue in (b) and (d). The electrodes (orange lines) were placed at an angle of 15° with respect to the retinal surfaces. When the electrodes were placed parallel with the axon bundles (a,b), only nearby RGCs were stimulated. However, the activation patterns spread to a much larger area when the electrodes were perpendicular to the axon bundles (c,d). Anodic-first biphasic pulses with pulse duration of 0.1 ms and current amplitude of 500 µA were used in both electrode configurations.

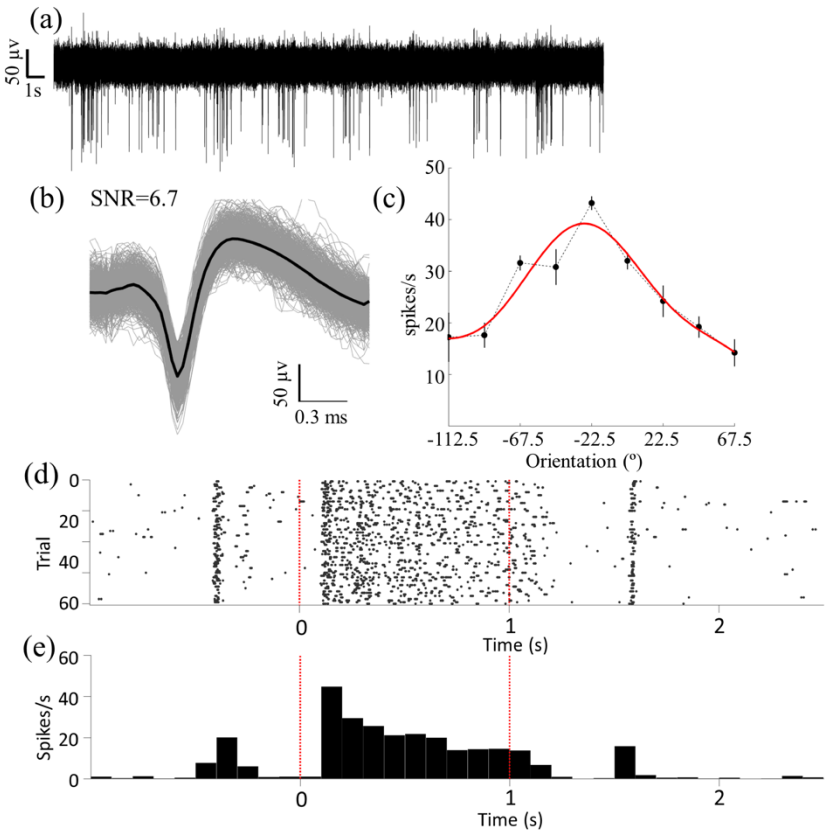

Figure 5. B-CNW coated CF electrodes could record in vivo single-units from wallaby visual cortex. (a) A thirty-second section of the neuronal response recording. (b) Individual spike waveforms (grey traces) and the mean spike waveform (black traces) from the single-unit recorded with a signal-to-noise ratio (SNR) of 6.7. (c) Orientation tuning responses of the single unit (black; SEM). The tuning was fit with a polynomial best fit curve (red). (d) Raster plot containing the responses of the single unit to sixty trials of a 3.5 s segment of a moving grating pattern The red dotted lines at zero show the onset and at 1s the offset of the moving grating. (e) Post-stimulus time histogram from the single unit with bins of 0.1 s. Time at zero is stimulus onset (first red dotted line) and stimulus offset 1s after (second red dotted line). The X and Y axes represent time (s) and spike rate (spikes/s), respectively. Time at -0.5s is the onset of the static grating and time of 1.5 s the offset of the static grating, which explains the synchronized spikes at those times in (d) and (e).

Table 1. A range of other commonly used neural interfacing electrode materials compared with B-CNW coated CF electrodes.

Types of material		*GSA* [μm^2]	Pulse width [μs]	*CIC* [$mC\ cm^{-2}$]	Impedance at 1 kHz [kΩ]	Water-Window [V]	Reference
CF with coatings	Iridium oxide coated CF	385±55 or 600	500	17 (0.6V bias); 1 (0V bias)	57	-0.6~0.6	[6b]
	PEDOT:PSS-co-MA coated CF	5472	200	25.91	~5	-0.9~0.4	[2e]
	N-UNCD coated CF	3220	500	7.09±3.65	~25	-1.8~1.2	[9]
	B-CNW coated CF	3220	500	7.82±0.35	28.8±4.2	-1.8~1.2	This work
Other microfiber electrodes	Reduced graphene oxide fiber	1256-1963	500	14±0.9	~5	-1~0.9	[24]
	Carbon nanotube fiber	1450	60	6.5	11.2±7.6	-1.5~1.5	[2d]
	Graphene fiber	169 ± 25	100	10.34	1900±300 [$K\Omega\ \mu m^{-2}$]	-1~0.9	
	Uncoated CF	2238	500	0.024±0.008	133.4±10.1	-0.4~0.6	This work
Commonly used planar electrodes	Pt	7850	200	0.2	54	-0.6~0.8	[31]
	TiN	4000	500	0.9	-	-0.9~0.9	[23b]
	Carbon	5700	1000	1-1.6	~2	-1.5~1	[32]

	nanotube						
	PEDOT:PSS	4500	200	2.92	27	-0.6~0.8	[33]

Table of Contents

Boron-doped carbon nanowalls are deposited on individual carbon fiber microelectrodes. The coated electrodes exhibit flexibility, stability, biocompatibility and greatly enhanced electrochemical properties. They can evoke localized neural responses and sense high quality signals from single neurons. They are suitable for long-term application in the future generation of closed loop neuromodulatory implants.

Keyword carbon fiber, carbon nanowall, implantable, stimulation, recording

Maryam A. Hejazi, Wei Tong, Alastair Stacey, Shi H. Sun, Molis Yunzab, Ali Almasi, Young Jun Jung, Hamish Meffin, Kate Fox, Khatereh Edalati, Athavan Nadarajah, Steven Prawer, Michael R. Ibbotson, David. J Garrett*

High Fidelity, Bidirectional Neural Interfacing with Carbon Fiber Microelectrodes Coated with Boron-doped Carbon Nanowalls: an Acute Study